Inorg. Chem. **2006**, *45*, 1270−1276

Insight into Framework Destruction in Ultramarine Pigments

Eleonora Del Federico,[†] Wolfgang Shöfberger,[‡] Johannes Schelvis,[‡] Sofia Kapetanaki,[‡] Lindsey Tyne,[†] and Alexej Jerschow*[,‡]

Department of Mathematics and Science, Pratt Institute, 200 Willoughby Ave, Brooklyn, New York 11205, and Department of Chemistry, New York University, New York, New York 10003

Received June 3, 2005

We report key evidence on the framework destruction in ultramarine pigments upon color fading. Experiments on faded pigments in a fresco painting environment reveal that the paramagnetic chromophores are set free via sodalite framework destruction and are subsequently degraded. Fading in acidic media produces similar results, although a larger number of β-cages appear to be destroyed, and H_2S is released. The findings are further supported by studies on natural and synthetic ultramarine pigments of various shades via solid-state resonance-Raman spectroscopy, colorimentry, and solid-state ^{29}Si and ^{27}Al NMR spectroscopy. NMR parameters are shown to correlate well with the intensities of Raman signals corresponding to the $S_3^{-\bullet}$ chromophores. A further correlation is established between the colorimetric parameters, L^* (lightness) and C^* (chroma), and the paramagnetic shift and paramagnetic linebroadening in NMR spectra for both ^{27}Al and ^{29}Si.

Introduction

The natural ultramarine pigment, obtained from the semiprecious stone lapis lazuli, has been one of the most valued pigments by European painters since the late 13th century when it was officially introduced to Europe by Marco Polo.[1,2] Lapis lazuli provided not only a vibrant blue color unmatched by any other pigment available at the time, but it added a divine nature to the artwork in which it was used. Since it was valued more highly than gold, its use typically conveyed the high status of the commissioner. Ultramarine was the pigment often reserved to paint the robes and mantel of Jesus and the Virgin, whereas less precious blues such as Smalt (a potassium and cobalt glass) or Azurite ($CuCO_3 \cdot 2Cu(OH)_2$) were used for the sky and other less heavenly characters. Lapis lazuli is often assumed to be fresco compatible and, therefore, stable in the presence of the highly alkaline lime mortar,[3] a mixture of sand and calcium hydroxide. However, Medieval and Renaissance treatises often advise to mix ultramarine with a proteinaceous binding medium, such as gelatin, and to paint over dry mortar.[4−6] Even the great Michelangelo, a strict fresco painter, who considered adding a binding medium an inferior fresco technique,[3,7,8] seemed to have followed the advise. During the restoration of the Sistine Chapel's "Last Judgment", an extra layer of ultramarine mixed with an organic medium was revealed on top of a pure ultramarine and mortar layer, [8,9] suggesting that Michelangelo may have compromised his beliefs in order to achieve the right intensity of blue color required for his masterpiece.

From a conservation standpoint, instances of fading of ultramarine pigments in paintings have been reported.[1,10,11] To date, the causes of color alteration of ultramarine pigments

* To whom correspondence should be addressed. E-mail: alexej.jerschow@nyu.edu.
[†] Pratt Institute.
[‡] New York University.

(1) Ashok Roy, E. *Artist's Pigments, A handbook of their history and characteristics*, 2nd ed.; National Gallery of Art, Oxford Unversity Press: 1993; Vol. 2, p 231.
(2) Reinen, D.; Lidner, G.-G. The nature of the chalcogen colour centres in ultramarine-type solids. *Chem. Soc. Rev.* **1998**, *28*, 75−84.
(3) Cather, S. *The Conservation of wall paintings: proceedings of a symposium organized by the Courtauld Institute of Art and the Getty Conservation Institute, London, July 13−16, 1987*; Getty Conservation Institute: Marina del Rey, CA, 1991; p 148.
(4) Merrifield, M. P., *Medieval and Renaissance treatises on the Arts of Painting*, 1999 ed.; Dover Publications: Mineola, NY, 1999; Vol. 1, p 918.
(5) Merrifiled, M. P. *The Art of Fresco Painting in the Middle Ages and the Renaissance*; Dover Publications: Mineola, NY, 2004; Vol. 1, p 192.
(6) Cennini, C. d. A. *The Craftsman's Handbook: "Il Libro dell' Arte"*; Dover Publications: Mineola, NY, 1954; Vol. 1, p 142.
(7) Vasari, G. *Vasari on Technique*; Dover Publications: Mineola, NY, 1960; Vol. 1.
(8) Chierici, S. *Michelangelo-the Last Judgment: a glorious restoration*; Abrandale Press, Harry N. Abraham, Inc.: New York, 1997.
(9) Vecchi, P. D. *The Sistine Chapel, a glorious restoration*; Harry N. Abraham, Inc.: New York, 1994.

10.1021/ic050903z CCC: $33.50
Published on Web 01/06/2006

are not yet completely understood. In this work, we report mechanistic evidence leading to ultramarine fading in both alkaline and acidic media.

Lapis lazuli's synthetic counterpart was first synthesized in 1828 by furnacing kaolin, sodium carbonate, and sulfur in an oxygen-free atmosphere.[1,12] By controlling the furnacing temperature and mixture composition, different colors of the pigment (blue, turquoise, green, violet, pink) became available.[13] Although natural ultramarine is no longer widely used, the synthetic ultramarine pigments are very important not only as artist's pigments but also as colorants in coatings, plastics, and various industrial materials.

Ultramarine pigments are aluminosilicates characterized by a sodalite framework with the generic formula $[Al_3Si_3O_{12}]^{3-}$ (also known as the "β-cage"). Paramagnetic ($S_3^{-\bullet}$, $S_2^{-\bullet}$) and diamagnetic (believed to be S_4 or S_3Cl) guests are located inside the cages and are responsible for the color of these pigments.[13] Negative charges are generally balanced by Na^+ cations, which are also inside the cages.[14] Although many studies have been published about the aluminosilicate framework structure,[14−17] scarce information is available on the chromophore concentration and occupancy.[18]

It has previously been shown that the resonance-Raman (RR) signal intensity of the $S_3^{-\bullet}$ signal at 548 nm can be correlated well with the color strength.[19] Furthermore, an EPR index via the observation of the $S_3^{-\bullet}$ signal has been established, where the EPR intensity shows a good correlation with the color strength.[19] The UV/vis and FTIR spectra, on the other hand, appear to be too complex to be interpreted. We used solid-state NMR spectroscopy in our study for providing a correlation between the spectroscopic parameters and the colorimetric parameters and for monitoring the structural changes upon pigment degradation. It has been reported that clustering of guests in neighboring cages can be diagnosed in sodalites via solid-state NMR studies.[20,21] In addition, NMR provides the opportunity to monitor the effect of diamagnetic guests in the cages, which is particularly important in the cases of pigment fading.

Solid-state NMR is an ideal technique for the study of these systems as it provides detailed information on the local structure around the observed nuclei in the form of chemical shifts and, for nuclei with spins larger than 1/2, quadrupolar couplings.[22] In addition, the paramagnetic guests of the sodalite framework create paramagnetic shifts, as well as line-broadening[23] effects, which we used in these studies as indicators of chromophore concentrations. We have applied ^{27}Al and ^{29}Si MAS NMR to study ultramarine pigments of different colors and their degradation products by lime mortar and acids.

Experimental Section

Ultramarine Pigments. The synthetic ultramarine pigments were obtained from Kremer Pigments, New York, NY. Eight different synthetic shades were used, blue D (dark), BD; blue R (reddish), BR; blue G (greenish), BG; violet RD (reddish dark), VRD; violet RL (reddish light), VRL; violet M (medium), VM; green, G (a gift from Dr. Gregor Kremer); red, R, and one mineral pigment, lazurite, the main blue mineral in lapis lazuli. This last sample was obtained from Zecchi Pigments, Florence, Italy. The slaked lime, aged $Ca(OH)_2$, used in the preparation of lime mortar was also obtained from Kremer pigments and the silica sand form Aldrich.

Resonance-Raman (RR) Spectroscopy. The RR spectra were obtained using the system described previously.[24] The samples were contained in an EPR tube and were excited with 406.7 and 530.9 nm light from a Kr^+ laser (Coherent, I-302) in a backscattering sample geometry. A cylindrical lens ($f = 150$ mm) was used to focus the laser beam onto the sample with an incident laser power of 10 mW. Rayleigh scattering was rejected using appropriate holographic notch filters (Kaiser Optical). The $S_3^{-\bullet}$ (548 and 1096 cm^{-1}) and $S_2^{-\bullet}$ (587 and 1169 cm^{-1}) chromophores were excited at 406.7 nm, and the red chromophore (S_4 or S_3Cl: 653, 675, and 1029 cm^{-1}) was excited at 530.9 nm. The more optimal excitation wavelength of 457.9 nm was not available in our setup. Background correction of RR spectra was done by subtraction of a smooth polynomial; toluene was used to calibrate the RR spectra, and sodium nitrate was added to the samples as an internal standard for calibration of the signal intensities. The spectra were normalized on the 186 cm^{-1} peak of sodium nitrate followed by a correction for the weight/weight percentages of the different pigments and sodium nitrate.

Solid-State NMR. NMR experiments were performed on a Bruker AV 400 MHz solid-state NMR spectrometer (9.4 T) using a 4 mm MAS rotor. The single-pulse experiments were performed

(10) Bosshard, E. D. In *Discoloration of Synthetic Ultramarine A Case History*; ICOM Commitee for Conservation, 5th Triennial Meeting, Zagreb, 1978; Zagreb, 1978; pp 78/6/2/1−78/6/2/4.

(11) Boissonnas, P. A treatment for blanching paintings. *Stud. Conserv.* **1977**, *22*, 43−44.

(12) Gobeltz, N.; A.Demortier; Lelieur, J. P.; Duhayon, C. Encapsulation of the chromophores into the sodalite structure during the synthesis of the blue ultramarine pigment. *J. Chem. Soc., Faraday Trans.* **1998**, *94*, 2257−2260.

(13) Clark, R. J. H.; Dines, T. J.; Kurmo, M. On the Nature of the Sulfur Chromophores in Ultramarine Blue, Green, Violet, and Pink and of the Selenium Chromophore in Ultramarine Selenium: Characterization of Radical Anions by Electronic and Resonance Raman Spectroscopy and the Determination of Their Excited-State Geometries. *Inorg. Chem.* **1983**, *22*, 2766−2772.

(14) Barrer, R. M., *Hydrothermal Chemistry of Zeolites*; Academic Press: London, New York, 1982; p 360.

(15) Hassan, I.; R. C.Peterson; Grundy, H. D. The Structure of Lazurite, Ideally $Na_6Ca_2(Al_6Si_6O_{24})S_2$, a Member of the Sodalite Group. *Acta Crystallogr.* **1985,** *C41*, 827−832.

(16) Klinowski, J.; Tarling, S. E.; Barnes, P. The Structure and Si, Al Distribution of the Ultramarines. *Acta Crystallogr.* **1988**, *B44*, 128−135.

(17) Klinowsi, J.; W.Carr, S.; Tarling, S. E.; Barnes, P. Magic-angle-spinning NMR shows the aluminosilicate framework of ultramarine to be disordered. *Nature* **1987**, *330*, 56−58.

(18) Gobeltz-Hautecoeur, N.; A.Demortier; Lelieur, J. P.; B.Lede; Duhayon, C. Occupancy of the Sodalite Cages in the Blue Ultramarine Pigments. *Inorg. Chem.* **2002**, *41*, 2848−2854.

(19) Gobeltz, N.; A.Demortier; Lelieur, J. P.; Duhayon, C. Correlation between EPR, Raman and colorimetric characteristics of the blue ultramarine pigments. *J. Chem. Soc., Faraday Trans.* **1998**, *94*, 677−681.

(20) Heinmaa, I.; Vija, S.; Lippmaa, E. NMR study of antiferromagnetic black sodalite $Na_8[AlSi_4]_6$. *Chem. Phys. Lett.* **2000**, *327*, 131−136.

(21) Trill, H.; Eckert, H.; Srdanov, V. I. NMR study of interacting F centers in $Na_8[Al_6Si_6O_{24}]Cl_2$ sodalite. *Phys. Rev. B* **2005**, *71*, 014412-1−014412-6.

(22) Laws, D. D.; Bitter, H. M. L.; Jerschow, A. Solid-state NMR methods in chemistry. *Angew. Chem., Intl. Ed.* **2002**, *41*, 3096−3126.

(23) Nayeem, A.; Yesinowski, J. P. Calculation of magic-angle spinning nuclear magnetic resonance spectra of paramagnetic solids. *J. Chem. Phys.* **1988**, *89*, 4600−4608.

(24) Schelvis, J. P. M.; Ramsey, M.; Sokolova, O.; Tavares, C.; Cecela, C.; Connell, K.; Gindt, Y. M. Resonance Raman and UV−vis Spectroscopic Characterization of the Complex of Photolyase with UV-damaged DNA. *J. Phys. Chem. B* **2003**, *107*, 12352-1362.

Table 1. Normalized Raman Intensities of Spectra Taken at 530.9 nm Excitation Wavelength[a]

pigment type	ID	$S_2^{-\bullet}$ 587 cm^{-1} normalized intensity	$S_3^{-\bullet}$ 548 cm^{-1} normalized intensity	S_4 or S_3Cl 675 cm^{-1} normalized intensity
red (R)	Kremer 42060	0	73.5	690
blue reddish (BR)	Kremer 45020	190	3530	0
blue greenish (BG)	Kremer 45030	180	4330	0
blue dark (BD)	Kremer 45000	195	5040	0
violet reddish light (VRL)	Kremer 45120	32	880.00	910
violet reddish dark (VRD)	Kremer 45110	56	1360	707
lapis lazuli (L)	Zechi 2002	28	605	13
violet medium (VM)	Kremer 45100	67	1215	290
green (G)	Kremer 00001	105	1840	0

[a] The $S_2^{-\bullet}$ signal was below the sensitivity threshold for the R sample.

at 10 kHz magic-angle-spinning (MAS) at room temperature. The 90° pulse lengths were approximately 5.2 μs for ^{29}Si, and 4 μs for ^{27}Al. The repetition delay was 1 s for the ^{29}Si MAS experiments and 10 s for the ^{27}Al MAS experiments. Chemical shifts are reported with respect to 0.1 M $Al(NO_3)_3$ for ^{27}Al and TMS for ^{29}Si. One thousand twenty four data points were acquired to cover a spectral window of 50 kHz. The numbers of transients accumulated were typically 40 for ^{27}Al, and 1000 for ^{29}Si.

Colorimetry. The reflectance experiments were performed using a Minolta Chroma Meter CR-300 colorimeter. The visible spectra were obtained from the reflectance data using the Kubelka−Munk transform. The color of the different ultramarine pigments was determined using the CIELAB 1976 space,[25] which organizes color so that numerical differences agree consistently with visual perceptions. In the CIELAB color system, the coordinates are L^*, lightness; a^*, the red-green coordinate; and b^*, the yellow-blue coordinate. In addition, colors can also be described using the cylindrical coordinates L^*, C^* (Chroma), and h^* (hue). Lightness measures the ability of the sample to transmit diffusely the incident light so that $L^* = 100$ for a white sample and $L^* = 0$ in a black sample. The chroma, C^*, coordinate is perpendicular to L^* and is calculated as $C^* = [(a^*)^2 + (b^*)^2]^{1/2}$, and it represents the amount of chromatic component in the pigment (as opposed to achromatic or gray). The hue is an angle, also calculated from a^* and b^* and given by the expression $h^* = \arctan(b^*/a^*)$. The a^* and b^* values were obtained from the reflectance spectra using the standard equations defined by the Commission Internationale de l'Eclairage (CIEDLAB 1976).[25] The granulometry data are available for all samples except the red and the green pigments and lapis lazuli. The sizes are: DB, 3.4; BR, 2.6; BG, 0.7; VRD, 1.9; and VRL, 1.5 μm. Since the particle size is nonuniform, as is typical for these industrial pigments, we expect some dispersion arising from the reflectometry data.

For the colorimetric measurements, equal amounts of pigments (500 mg) were mixed with 1 mL of distilled water and then applied over a lime mortar layer (a mixture of 50% w/w of slaked lime-colloidal $Ca(OH)_2$ and 50% of silica sand) that was allowed to dry for a week at 40% relative humidity.

Preparation of Faded Pigments. Pigments were degraded by two different procedures involving (a) lime mortar, which simulates a fresco-painting environment, and (b) exposure to 3.0 M HCl. In procedure (a), 500 mg of each pigment is mixed with 1 mL of distilled water and then applied over a lime mortar layer that was previously prepared over a ceramic tile. The simulated fresco painting is then stored in a chamber at 85% RH for 2 weeks. After that time, all pigments completely fade, except for the ultramarine green, which turns yellow. NMR samples are collected by carefully scraping off the degraded pigment layer using a scalpel. In procedure (b), 1 g of each pigment is placed in a test tube and 4 mL of 3.0 M HCl is added. The fading of the pigments occurs within 1 min with the emission of H_2S. The faded pigments are then suction filtrated, rinsed with distilled water, and dried at 40% RH for one week. At that point, they are ground and ready for NMR measurements.

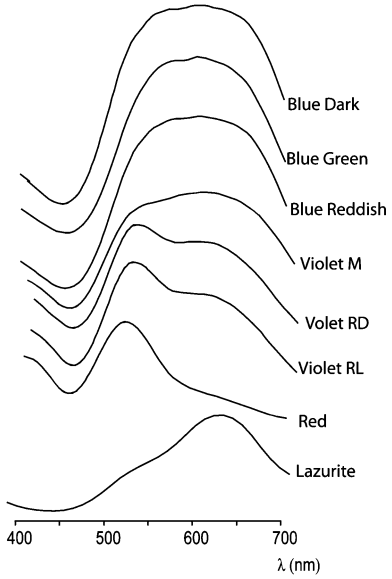

Figure 1. Visible spectra of the ultramarine pigments obtained using the Kubelka−Munk transform from the reflectance spectra.

Table 2. Colorimetric Parameters for the Different Ultramarine Pigments

pigment type	h^* (hue)	L^* (lightness)	C^*(Chroma)
red (R)	346	67	28
blue reddish (BR)	292	35	72
blue greenish (BG)	278	36	72
blue dark (BD)	284	28	75
violet reddish light (VRL)	293	46	47
violet reddish dark (VRD)	299	47	41
lazurite (L)	251	67	32
violet medium (VM)	283	41	53

Results and Discussion

The normalized Raman intensities (530.9 nm) for the different pigments are reported in Table 1. Figure 1 shows the reflectance spectra of the pigments. The colorimetry parameters were calculated from these spectra and summarized in Table 2. The synthetic blue pigments have the strongest absorbance, lowest lightness (L^*) parameters, and highest chroma (C^*). The blue pigments contain mostly the

(25) Wyszecki, G.; Stiles, W. S. *Color Science, Concepts and Methods, Quantitative Data and Formulae*, 2nd ed.; John Wiley and Sons: New York, 2000.

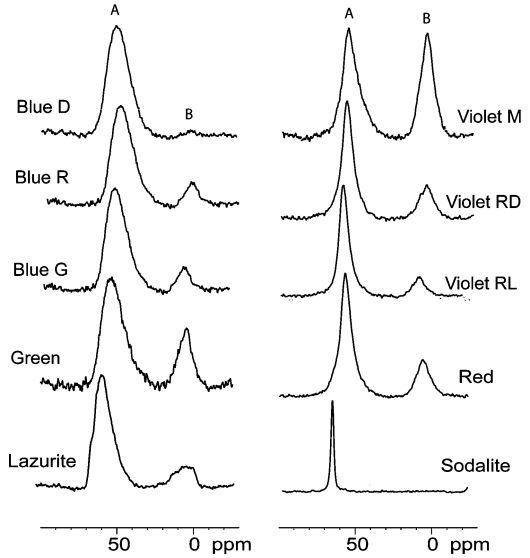

Figure 2. ^{27}Al MAS NMR spectra of the ultramarine pigments. The spectrum of sodalite is included for comparison.

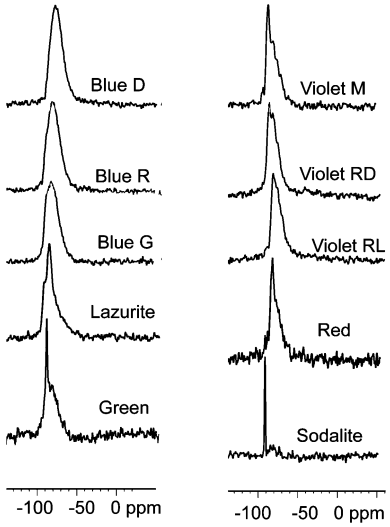

Figure 3. ^{29}Si MAS NMR spectra show the resonances of the blue pigments being right shifted and broader than the violet and red pigments. The sodalite spectrum is included for comparison.

$S_3^{-\bullet}$ chromophores with smaller amounts of $S_2^{-\bullet}$.[19] Therefore, the lightness of the pigments seems to decrease with higher concentrations of these chromophores, whereas the chroma increases in the sense that it displays high lightness and low chromaticity. It is perceived as blue because $S_3^{-\bullet}$ is the most abundant chormophore, and in comparison, the concentration of red chromophore (S_4 or S_3Cl) is negligible. In contrast, the violet pigments display considerably larger normalized Raman intensities for the red chromophore.

The RR experiments were performed at two different excitation wavelengths: 406.7 and 530.9 nm. The peaks at 548 and 1097 cm^{-1} are due to the $S_3^{-\bullet}$ chormophore, the peaks at 587 and 1169 cm^{-1} are assigned to the $S_2^{-\bullet}$ chromophore, and the peaks at 1029, 653, and 675 cm^{-1} to the red chromophore (S_4 or S_3Cl).[13,26,27] The Raman intensities for the peaks due to the $S_3^{-\bullet}$ chromophore are largest for the blue pigments in agreement with the assumption that these pigments have larger concentrations of these chromophores. In addition, the peaks assigned to the red chromophore are more intense for the violet and red pigments, implying a higher concentration of the red chromophore in these shades.

Figure 2 shows the ^{27}Al and Figure 3 the ^{29}Si MAS NMR spectra performed on these pigments. Both the ^{29}Si MAS and ^{27}Al MAS NMR spectra display similar trends. The resonance corresponding to the cages filled with paramagnetic guests is shifted in frequency due to the paramagnetic isotropic shifts.[20,21] $S_3^{-\bullet}$ has been shown to display *g*-anisotropy at low temperatures.[19] More recently, three different $S_3^{-\bullet}$ species have been identified in ultramarines which displayed different *g*-anisotropies at temperatures of 10 K and below and even at room temperatures.[28] It is assumed, however, that due to motional averaging the *g*-anisotropy can be neglected at room temperature and that the origin of the paramagnetic shift can be attributed to the Fermi-contact interaction, rather than a pseudo-contact shift.[23] The direction of this shift cannot easily be predicted.[23]

The ^{27}Al spectra, as opposed to the ^{29}Si spectra, display two peaks: a more-intense peak (A), that appears between 48 and 57 ppm (tetrahedral framework sites) and a less-intense peak (B) that remains at a constant chemical shift of about 0 ppm (octahedral nonframework sites). Peak B does not show any effects as a function of paramagnetic guest concentration, suggesting that it does not depend on the presence of paramagnetic species. Therefore, peak B can be assigned to extra-framework aluminum species. We note that kaolinite shows the same chemical shift as peak B, and it is reasonable to assume that the industrial pigments contain a significant fraction of this material. Peak A, which is strongly dependent on the blue shade of the pigments, was assigned to framework aluminum in the proximity of paramagnetic species, such as $S_2^{-\bullet}$ and $S_3^{-\bullet}$. Lapis lazuli also behaves as a violet ultramarine pigment in terms of NMR paramagnetic shift and linebroadening, indicating a lower concentration of the paramagnetic chromophores, which is in line with the RR spectra. In previous studies, similar NMR spectra were found for the antiferromagnetic black sodalite (however, with an opposite paramagnetic shift).[20]

The absence of a B-type peak in the ^{29}Si spectra is due to the lack of the large isotropic shift differences between the tetrahedral and octahedral configurations observed for ^{27}Al.

Another parameter diagnosing the paramagnetic guest concentration in the cages is the linebroadening, which increases with increasing paramagnetic host concentrations. This effect is likewise seen in both the ^{27}Al and ^{29}Si spectra. The linebroadening effect is most likely due to the electron−nuclear dipolar coupling mechanism.

(26) Clark, R. J. H.; Franks, M. L. The Resonance Raman Spectrum of Ultramarine Blue. *Chem. Phys. Lett.* **1975**, *34*, 69−72.
(27) Clark, R. J. H.; Cobbold, G. D. Characterization of Sulfur Radical Anions in Solutions of Alkali Polysulfides in Dimethylformamide and Hexamethylphosphoramide and in the Solid State in Ultramarine Blue, Green, and Red. *Inorg. Chem.* **1978**, *17*, 3169−3174.
(28) Arieli, D.; Vaughan, D. E. W.; Goldfarb, D. New synthesis and insight into the structure of blue ultramarine pigments. *J. Am. Chem. Soc.* **2004**, *126*, 5776−5788.

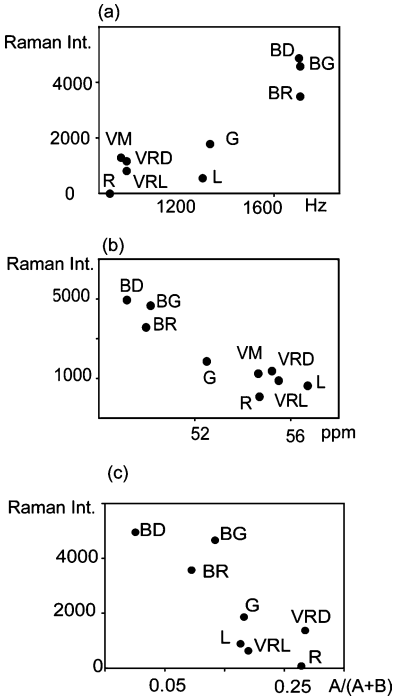

Figure 4. Correlations between the normalized Raman intensity at 548 cm^{-1} corresponding to the $S_3^{-\bullet}$ chromophore and (a) ^{27}Al line width, (b) ^{27}Al chemical shift (peak A), (c) integral ratio $A/(A + B)$.

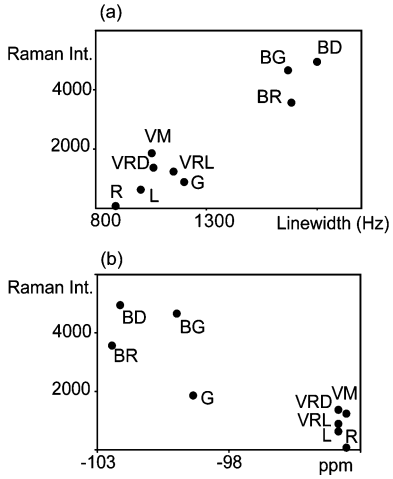

Figure 5. Correlations between the normalized Raman intensity at 548 cm^{-1} corresponding to the $S_3^{-\bullet}$ chromophore of all ultramarine pigments and their (a) ^{29}Si line width, (b) ^{29}Si chemical shift.

Above assignments can be verified in the following manner. We correlate both the paramagnetic shifts, as well as the line widths for both ^{27}Al and ^{29}Si as a function of $S_3^{-\bullet}$ content as determined via the normalized RR experiments. The results are shown in Figure 4 for ^{27}Al and Figure 5 for ^{29}Si. An increase in isotropic chemical shift, as well as an increase in line width correlates very well with the increased $S_3^{-\bullet}$ concentration for both nuclei. Similar correlations could not be established for the $S_2^{-\bullet}$ component, presumably because it shows weaker paramagnetic and dipolar interactions. It should be noted that an additional isotropic shift may arise from the quadrupolar interaction, which may give rise to a deviation from a perfect correlation.[29]

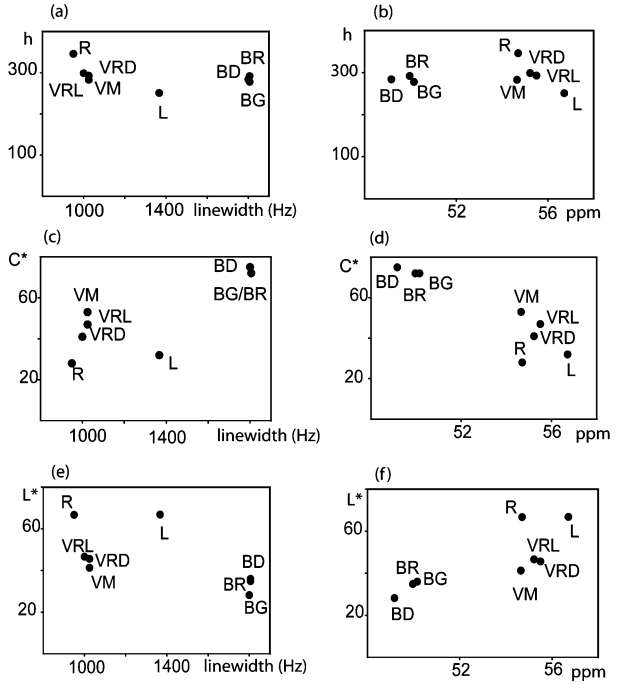

Figure 6. Correlations between the colorimetric parameters (*h*, *C**, and *L**) and the NMR parameters (line width and chemical shift for peak A in ^{27}Al MAS spectra): (a) *h* vs ^{27}Al line width, (b) *h* vs ^{27}Al chemical shift, (c) *C** vs ^{27}Al line width (d) *C** vs ^{27}Al chemical shift, (e) *L** vs ^{27}Al line width, (f) *L** vs ^{27}Al chemical shift.

For ^{27}Al, we further note that the expression $A/(A + B)$, where *A* and *B* stand for the integrals of peaks A and B, correlates reasonably well with the Raman signal for $S_3^{-\bullet}$. This fact cannot easily be interpreted, but the most likely explanation is that the fraction of paramagnetic cages correlates with the $S_3^{-\bullet}$ concentration. Due to the absence of a type-B peak in the ^{29}Si spectra, a similar comparison could not be made for ^{29}Si.

There is no noticeable line-splitting in the ^{27}Al spectra of peak A. This is an indication for the fact that cages of a given guest seem to be clustered in regions of "same-type cages" similar to two different solid phases (paramagnetic and diamagnetic) of the pigment coexisting together.[20] There is a slight indication of a distribution of different types of cages in the ^{29}Si spectra, where we notice both a sharp and a broad peak in the spectra of the G, VM, VRL, VRD, and R samples. However, the peaks could not be uniformly deconvoluted, which is why the overlapping signals were considered a single resonance peak. This is the most likely reason for the fact that the correlations involving ^{29}Si data seem slightly inferior to the ones of ^{27}Al. The isotropic shift and line width data suggest that we see an increase in the number of diamagnetic cages as the pigments become violet and pink.

Next, we correlate the NMR parameters with the colorimetric parameters *h*, *L**, and *C** in Figures 6 and 7. The *h* parameter appears not to vary over the range of chromophore concentrations studied, neither using ^{27}Al (Figure 6a) nor

(29) Jerschow, A. From nuclear structure to the quadrupolar NMR interaction and high-resolution spectroscopy. *Prog. Nucl. Magn. Reson. Spectroscopy* **2005**, *46*, 63−78.

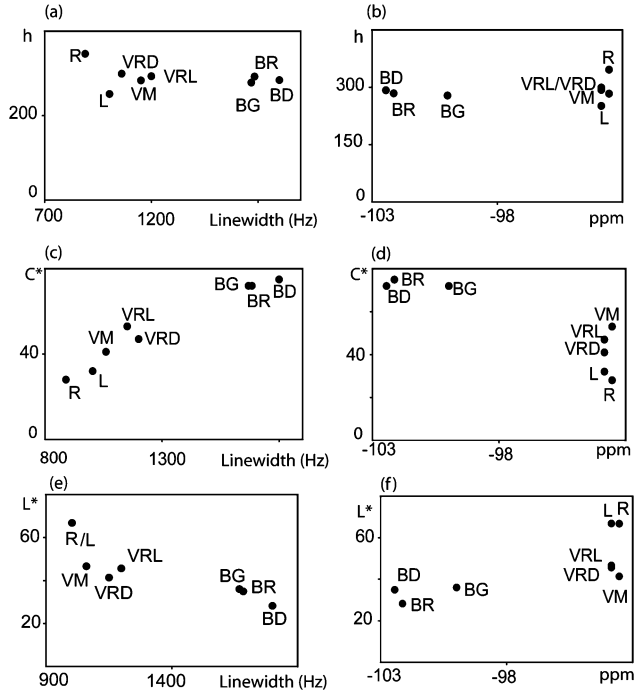

Figure 7. Correlations between the colorimetric parameters (*h*, *C**, and *L**) and NMR parameters (line width and chemical shift for peak A in ^{29}Si MAS spectra): (a) Correlation between *h* vs ^{29}Si line width, (b) *h* vs ^{29}Si chemical shift, (c) *C** vs ^{29}Si line width, (d) *C** vs ^{29}Si chemical shift, (e) *L** vs ^{29}Si line width, (f) *L** vs ^{29}Si chemical shift.

^{29}Si (Figure 7a) data. This indicates that the hue is determined by the presence of all three chromophores and not just $S_3^{-\bullet}$. On the other hand, the *C** and *L** parameters show a consistent correlation with the line width and the chemical shift of peak A in the ^{27}Al spectra and the line width and chemical shift of the single resonance peak in the ^{29}Si spectra. The correlation trend between *L** and *C** and the chemical shifts and line widths occurs in the same direction for both the ^{27}Al and ^{29}Si data: an increase of the concentration of the paramagnetic cages (measured by an increase in linebroading and a decrease of chemical shift) are associated with lower *L** and higher *C**. This is an indication that the colorimetric parameters *L** and *C** are determined mostly by the concentration of the blue chromophore $S_3^{-\bullet}$. This is in agreement with previous studies[19] finding that the color strength, a colorimetric parameter related to *L**, in ultramarine pigments is determined mostly by the concentration of $S_3^{-\bullet}$ measured via EPR. The dispersion of the colorimetric data can be attributed to the different granulometry of the pigments. As mentioned above, the pigments used in these studies are commercial grade, and therefore, the particle size distribution varies with the pigment shade. Nonetheless, reasonable correlations between the colorimetric parameters and both NMR parameters and Raman intensities can be obtained for $S_3^{-\bullet}$.

The faded pigments were investigated via ^{27}Al NMR, since ^{29}Si NMR showed significant background signals from the mortar matrix, and in general yielded very low intensity signals. The ^{27}Al NMR spectra of the faded pigments indicate a decrease of the concentration of paramagnetic cages, while the ratio of the intensities between peak B and peak A

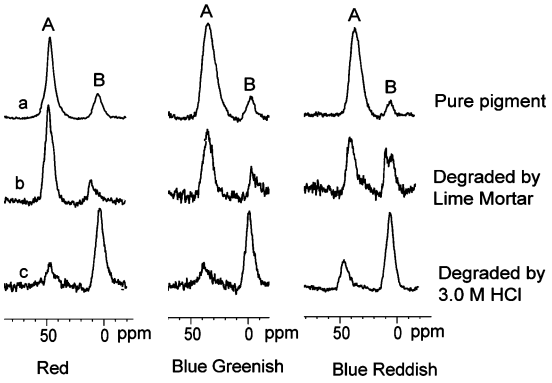

Figure 8. Comparison between the ^{27}Al MAS spectra for (a) the R, BG, and BR pigments, (b) the corresponding pigments faded by lime mortar (fresco), and (c) the corresponding pigments faded by the action of acid.

increases (Figure 8). At the same time, peak A becomes narrower and shifts to the left in the spectrum, consistent with a loss of paramagnetic chromophores. As mentioned above, peak B can be assigned to nonframework aluminum species. We have identified the resonance for sodalite (Figure 2), which is located at approximately 50 ppm downfield from the peak B resonances. Such large chemical shifts are unusual on the basis of a change of diamagnetic guest molecules in sodalites[30] but rather indicate a change of geometry or coordination; hence, simple guest-depletion (or paramagnet/diamagnet conversion) can be ruled out. In addition, Yoshida et al.[31] identified the signals of nonframework aluminum species at approximately the same chemical shifts as our peak B. Therefore, it can be concluded that the fading mechanism is due to aluminum framework destruction rather than in situ conversion of the chromophores. This also explains the absence of B-type peaks in the ^{29}Si spectra. In both the fresco environment and under acidic conditions, a yellow precipitate is found for the green ultramarine pigment, whereas the blue pigments turn gray in acidic medium and the violets turn white. Significant H_2S is also released during acidic degradation. It is assumed that both elemental sulfur, as well as sulfates, may be generated during degradation as well.[1] Efforts are underway to identify the chromophore degradation products in an alkaline medium.

Conclusions

The NMR data suggest that there is a substantial diamagnetic region, as well as a paramagnetic region, which do not mix to an appreciable extent. The paramagnetic NMR shifts correlate well with the $S_3^{-\bullet}$ Raman signals. The colorimetric parameters *L** and *C** correlate well with the paramagnetic shifts and linebroadenings, while the parameter *h* is rather unaffected. This is a strong indication that color in ultramarines is regulated via the concentration of paramagnetic species in the cages. These studies form the basis for the analysis of faded pigments in which the concentration of the major chromophores clearly decreases. In simulated fresco environments, these pigments lose their color and the NMR

(30) Fritzgerald, J. E. *Solid-state NMR spectroscopy of inorganic materials* American Chemical Society: Washington, DC, 1999.
(31) Yoshida, A.; Adachi, Y.; Inoue, K. Effect of nonframewrok alumina on the hydrothermal stability of USY. *Zeolites* **1991**, *11*, 549−552.

spectra show that the fraction of nonframework aluminum species increases. This is a clear sign of framework destruction accompanied by the release of the paramagnetic chromophores. These are subsequently degraded. In acidic environments, the free chromophores are converted largely to H_2S and possibly elemental sulfur, whereas the degradation product in alkaline medium remains to be identified. These studies explain for the first time the process of fading in ultramarines and may, besides providing this mechanistic information, lead to the design of proper art conservation treatments and the development of more-permanent pigments.

Acknowledgment. We thank Dr. Clare P. Grey, Dr. James P. Yesinowski, and Dr. Dieter Suter for helpful discussions on paramagnetic effects, Dr. Silvia Centeno and Ms. Emilia Cortes from the Metropolitan Museum of Art for allowing us to use the colorimetric equipment for these studies, Professor Licio Isolani for recommendations on the creation of the fresco paintings, Sally Pusede, Cyndi O'Hern, and Ken Girard for the sample preparation, Dr. Rene de la Rie for helpful discussions on ultramarine pigment degradation, and Dr. Mauro Bacci and Dr. Marcello Picollo for his helpful suggestions in the preparation of this manuscript. We are indebted to Dr. Gregor Kremer for providing us the green ultramarine samples and to Robert Gamblin for providing us with extra samples of blue ultramarines.

IC050903Z